Electronic Supplementary Material (ESI) for Journal of Materials Chemistry C
This journal is © The Royal Society of Chemistry 2013

Supplementary Information

# Synthesis of nitrogen-doped graphene by pyrolysis of ionic-liquid-functionnalized graphene

**Jen-Yu Liu‡[a], Hsin-Yun Chang‡[a], Quang Duc Truong[b], and Yong-Chien Ling*[a]**

[a] *Department of Chemistry, National Tsing Hua University, Hsinchu 30013, Taiwan.*

*E-mail: ycling@mx.nthu.edu.tw; Fax: +88635727774; Tel: +88635721484.*

[b] *Institute of Multidisciplinary Research for Advanced Materials, Tohoku University,*

*Sendai 980-8577, Japan*

‡These authors contributed equally to this work.

## Experiment

Two high-purity graphite rods were purchased from China National Medicines Shenyang Co. Ltd.. The ILs 1-butyl-3-methylimidazolium bromide ([Bimi][Br]), 1-butyl-3-methylimidazolium hexafluorophosphate ([Bmim][$PF_6$]) and 1-butyl-3-methylimidazolium acetate ([Bmim][Ac]), dimethyl sulfoxide (DMSO, 99%), ethanol ($C_2H_5OH$, 99%), hydrogen bromide (HBr, 99%) and ammonium ($NH_4OH$, 33%) were obtained from Fisher Scientific (USA). All stock solutions were prepared using deionized water without further purification. Two high-purity graphite rods were placed parallel with a separation of 1.0 cm, were inserted as electrodes into the electrolyte (IL: solvent = 1:10). AYJ26K model potentiostat (Yongheng Precision Ammeter Co., China) was used to provide the potential. Static potentials of 15V were applied to the two electrodes. After 3 hours, the anode graphite rod was exfoliated and then a black precipitate gradually appeared at the bottom of the reactor. The precipitate was washed by water and dried at 60 °C and thermal annealing in $N_2$ atmosphere for 4 h at 400 °C to obtain NG.

Transmission electron microscopy (TEM) images were obtained with a Hitachi model H-800 TEM opened at an accelerating voltage of 100 kV. XPS of the NG was obtained with a Physical Electronics Quantum 2000 scanning ESCA microprobe. AFM images were obtained with an atomic force microscope (Nanoscope III, Digital Instrument). The Raman spectra of the products were recorded at ambient temperature on a Raman spectroscopy (Horiba HR800, with laser excitation at 514.5 nm, 2 mW power). X-ray powder diffraction (XRD) measurements of the as-prepared sample were performed on a Rigaku D/max-IIB X-ray diffractometer with Cu Ka radiation ($\lambda$ = 0.15418 nm), and the electrochemical measurements were carried out at room temperature (25 ± 2 °C).

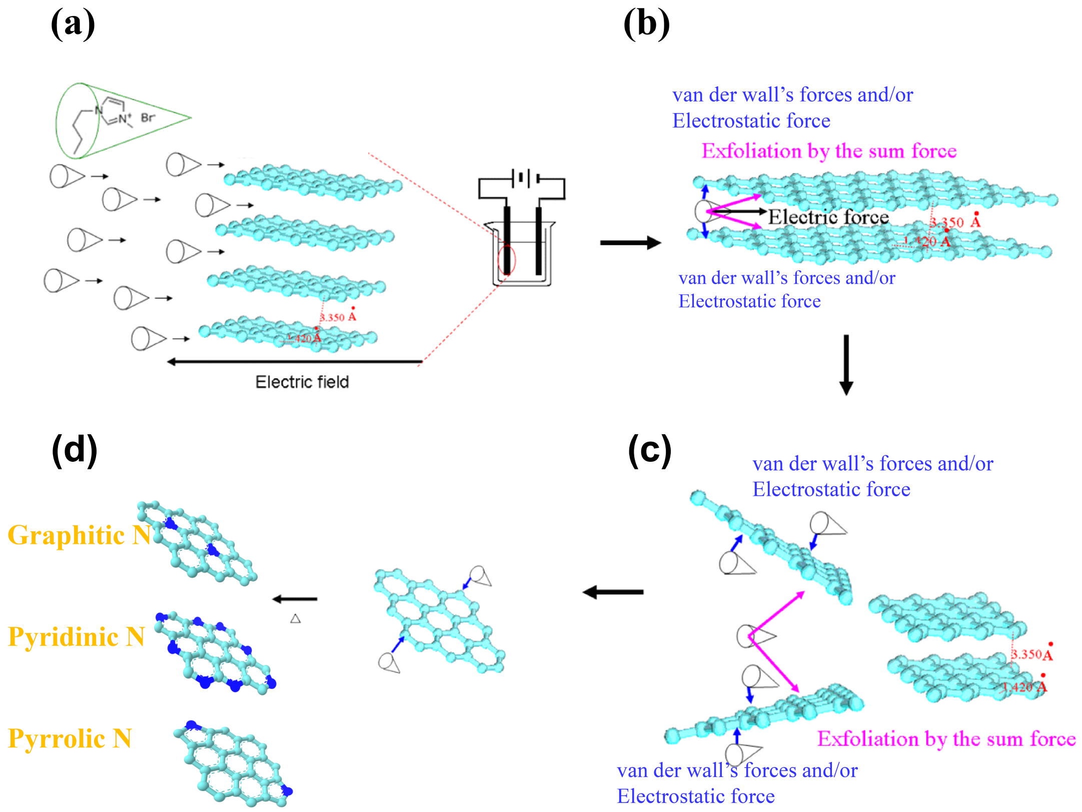

**Scheme S1.** Schematic of the synthesis of N-doped graphene from graphite: (a) Anions in ILs were pulled by anode; whereas cations in ILs were pulled to anode, (b) The cations were inserted into each layer of graphite and exfoliated by the summed force of electric force, Van der Wall's forces, and electrostatic force, (c) ionic-liquid-functionalized graphene was obtained, (d) Thermal annealing to yield NG with different N-doping configuration.

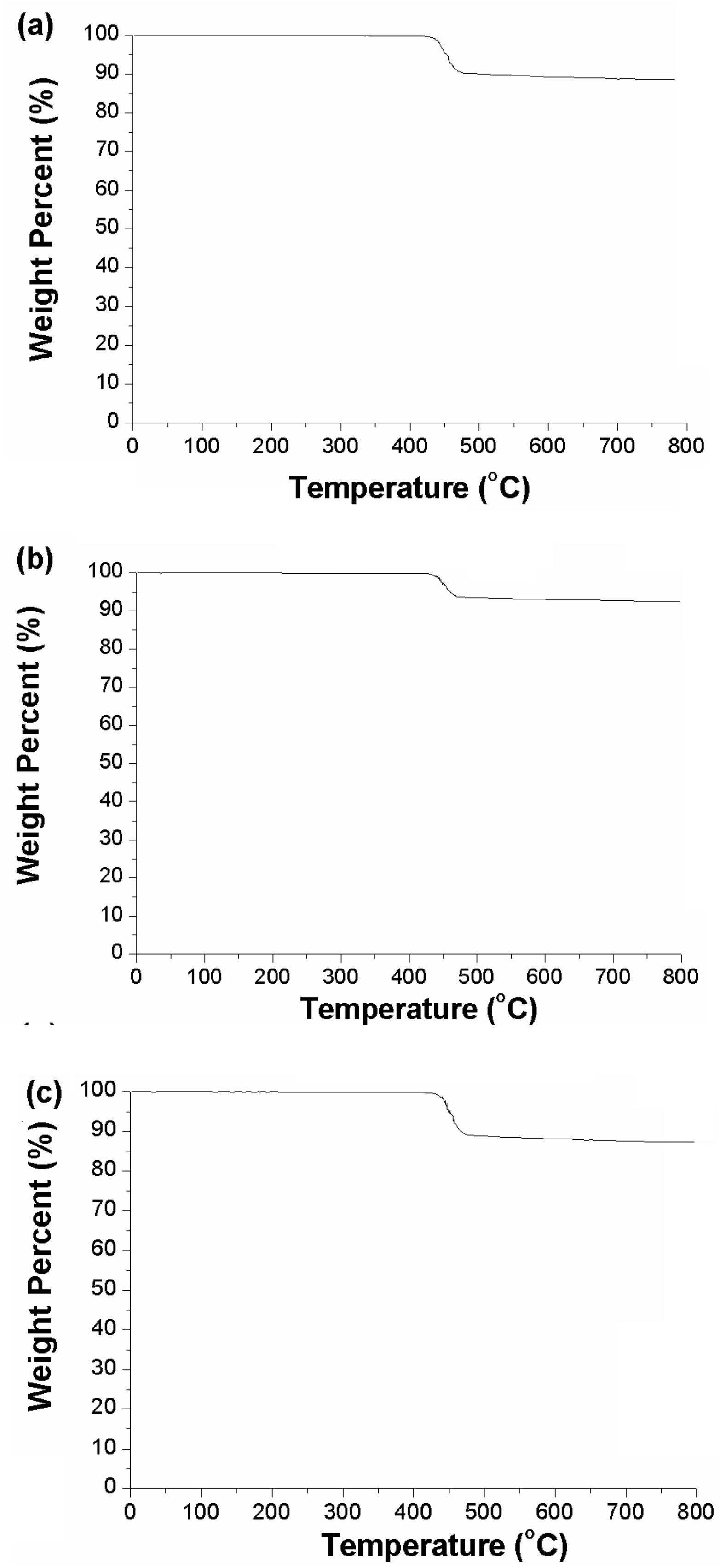

**Fig. S1.** TGA curve of N-doped graphene synthesized using (a) [Bmim]Br; (b) [Bmim][$PF_6$] and (c) [Bmim]Ac.

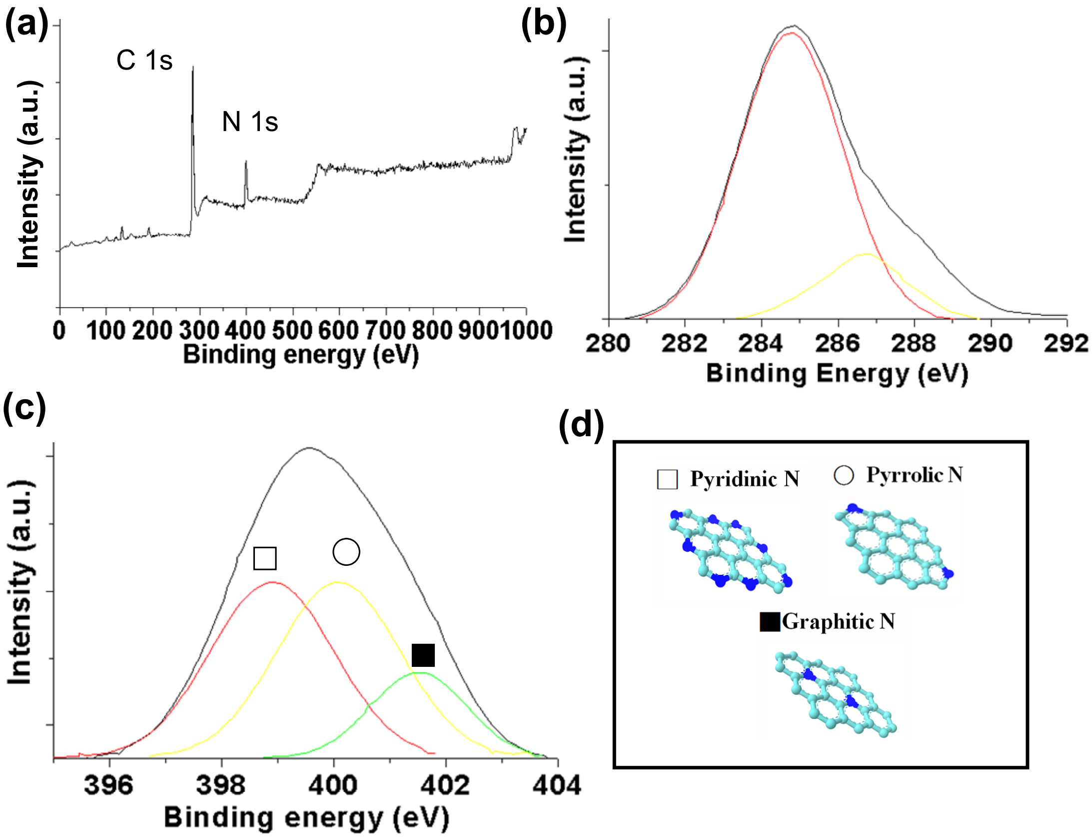

**Fig. S2** The XPS spectra of NG synthesized using [Bmim][$PF_6$] (a) Survey, (b) High resolution C 1s, (c) High resolution N1s, and (d) Schematic illustration of N-doping configurations.

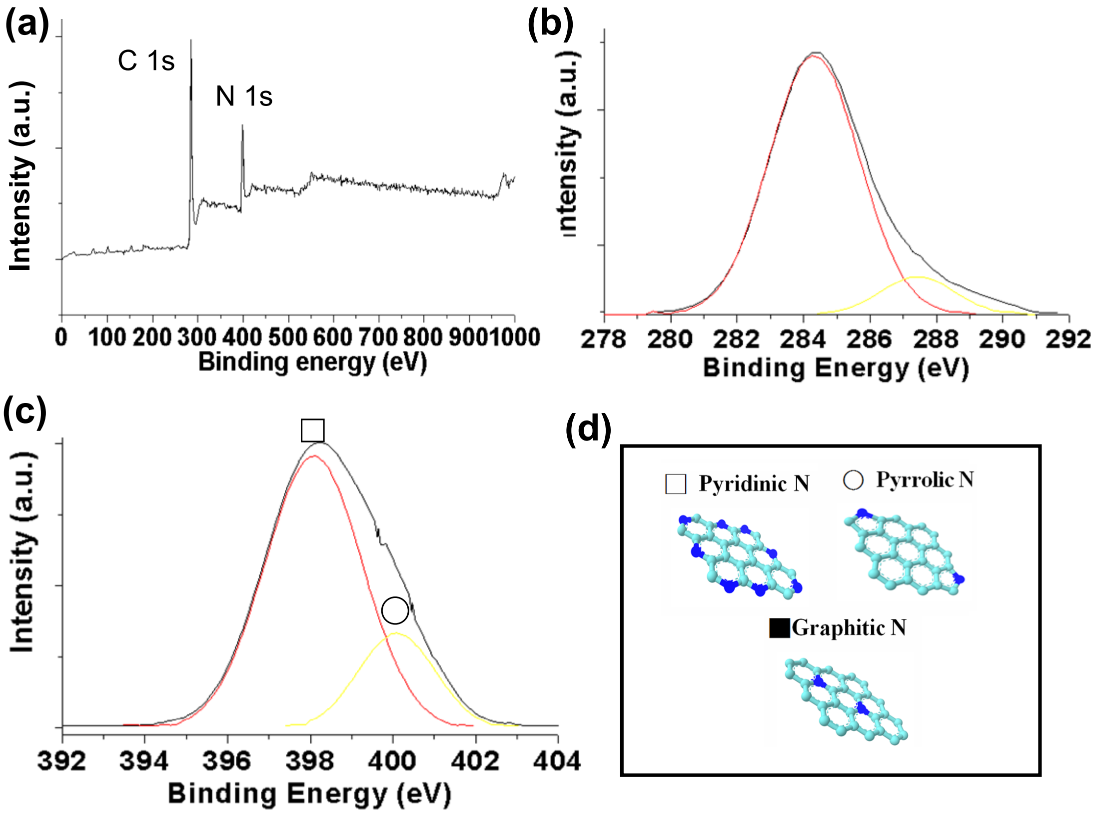

**Fig. S3** The XPS spectra of NG synthesized using [Bmim]Ac (a) Survey, (b) High resolution C1s, (c) High resolution N1s, and (d) Schematic illustration of N-doping configurations.

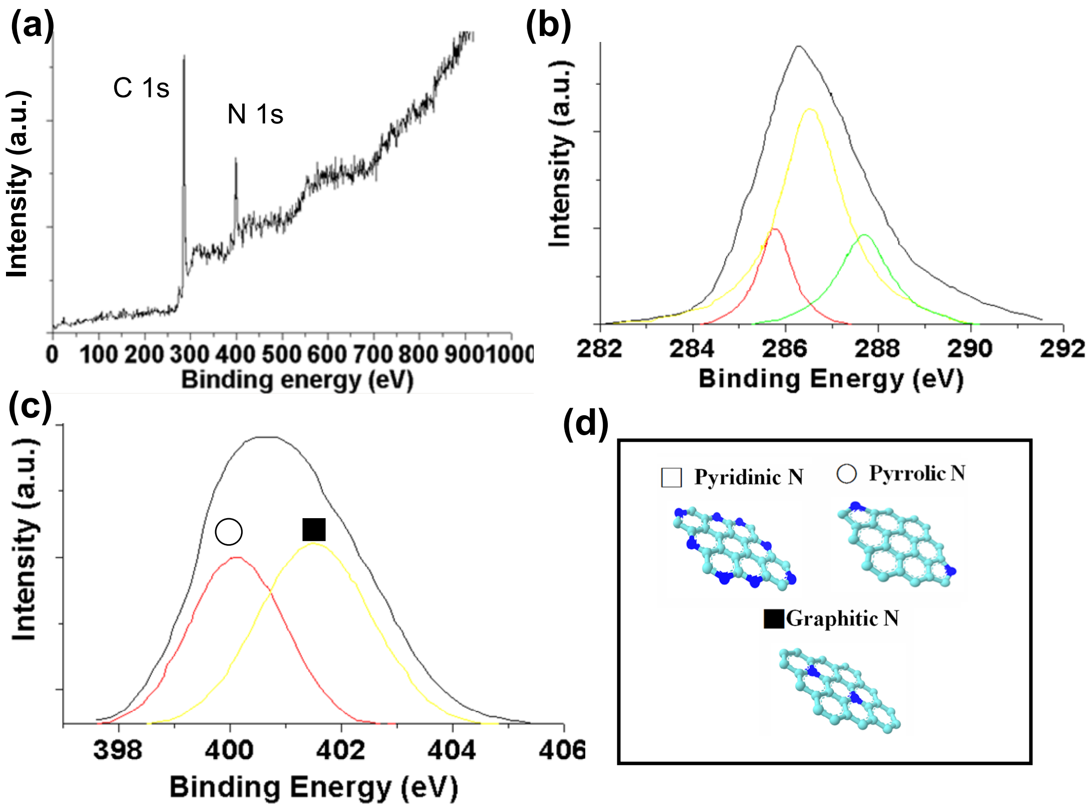

**Fig. S4** The XPS spectra of NG synthesized using [Bmim]Br in HBr at pH 2.0 (a) Survey, (b) High resolution C1s spectra, (c) High resolution N1s spectra, and (d) schematic illustration of N-doping configurations.

**Table S1**: The percentage of nitrogen/carbon in NG synthesized using (a) [Bmim][Br], (b) [Bmim][PF$_6$], and (c) [Bmim][Ac] determined by CHN analysis and XPS equation.

| ILs used | N/C (%) by XPS | N/C (%) by elemental analysis |
|---|---|---|
| [Bmim][Br] | 21.6 | 21.4 |
| [Bmim][PF$_6$] | 15.6 | 15.8 |
| [Bmim][Ac] | 22.1 | 21.9 |

## FTIR and NMR spectra of NG

The FTIR spectra (500–4000 cm$^{-1}$) were obtained using a Nicolet IR100 FTIR spectrometer. Generally, the graphite peak at about 3405 cm$^{-1}$ is related to the O-H stretching. The absorption peak at 1737cm$^{-1}$ is related to the C=O stretching of COOH groups at the edges of the GO sheets. The peak at 1627 cm$^{-1}$ is due to the H–O–H bending of absorbed water. The peaks at 1386 and 1057 cm$^{-1}$ are due to tertiary C-OH groups and C-O, respectively. The peaks of the N-doped graphene between 1647 cm$^{-1}$ can be asigned to the sp2 C=N and/or C=C, and the peak at 1259, 1393, and 1527 cm$^{-1}$ are related to the sp3 N-H.

High-resolution solid-state $^{13}$C NMR experiments were carried out on a JEOL ECA400 spectrometer operated at 100.53 MHz using the single-pulse decoupling method. The solid-state $^{13}$C NMR spectra with the $^{1}$H decoupling of graphite and N-doped graphene are measured. The graphite contains four peaks at 60, 70, 110, and 130 ppm, which are assigned to C-O-C epoxide groups, C-OH groups, and conjugated double bonds in oxidized aliphatic rings and aromatic entities, respectively. The N-doped graphene only contains one peak centered at 120 ppm, suggesting that aromatic entities have remained greatly.

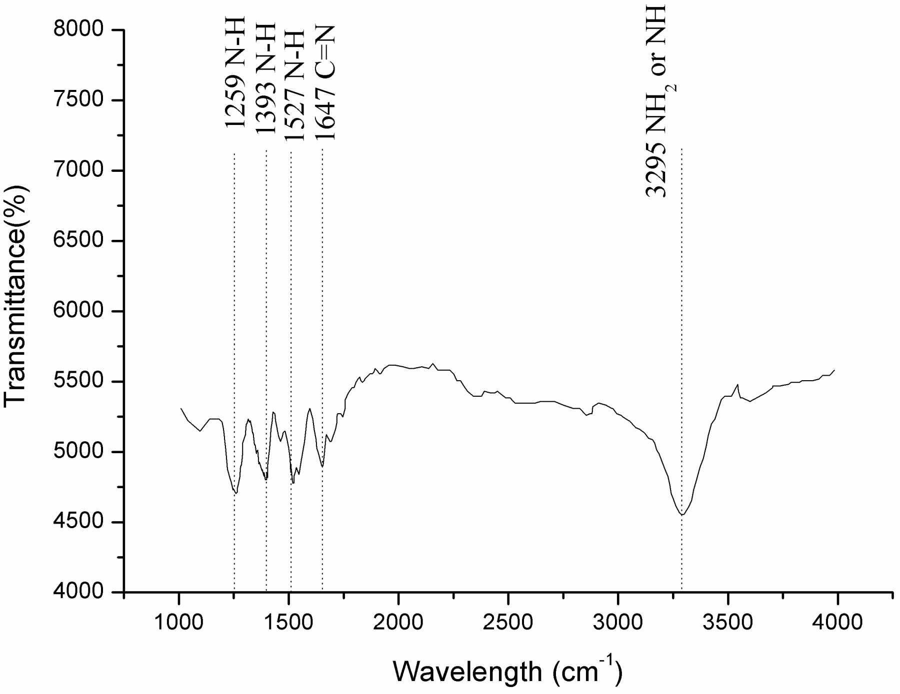

**Fig. S5** FTIR spectrum of NG synthesized using [Bmim][Br].

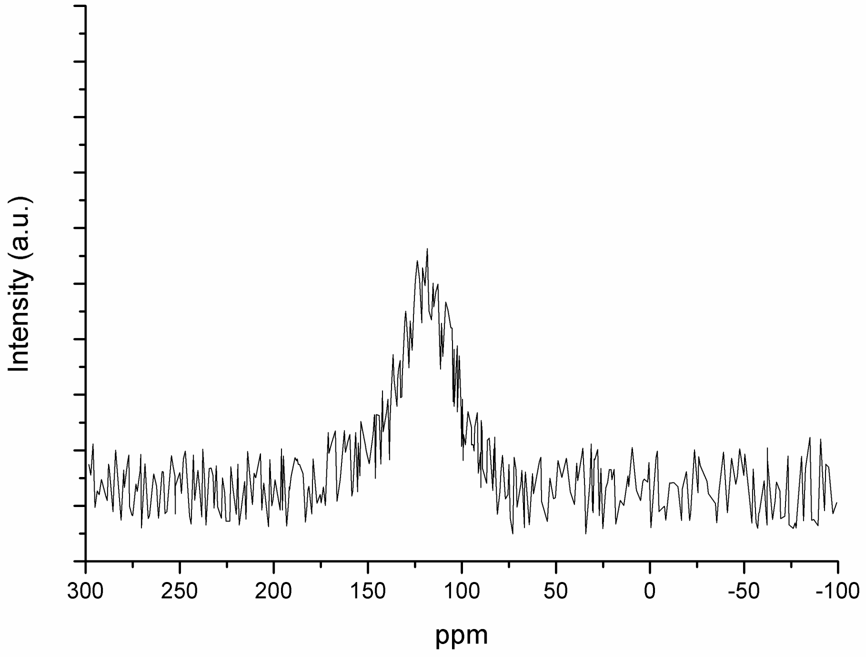

**Fig. S6** NMR spectrum of NG synthesized using [Bmim][Br].

## Raman

We calculated the Raman spectrum of nanoscale ordered structure to which Raman spectrum is sensitive with the package for first-principles computations ABINIT (URL http://www.abinit.org). Depending on the frequency of incident laser light we known the light scattering changed called as Raman effect by normal vibration on target molecular symmetry. The intensity and frequency of Raman spectrum varied with the lattice dynamics, such as phonon frequency, mass, and Raman tensor. We simulate the Raman spectrum with ABINIT, which is a joint project between the Universit´e Catholique de Louvain, Corning Incorporated, and other contributors. The first-principles calculation optimization was performed and finally damping constant ($\Gamma$i = 10 cm$^{-1}$), 8x8x1 Monkhorst-pack grid, ECUT=45 Ha and tolwfr = $10^{-18}$ were used. The disorder from O or N atoms insertion in the entire Brillouin zone determined the width of Raman bands with the corresponding phonon band.

## Raman shift simulation of D and G band

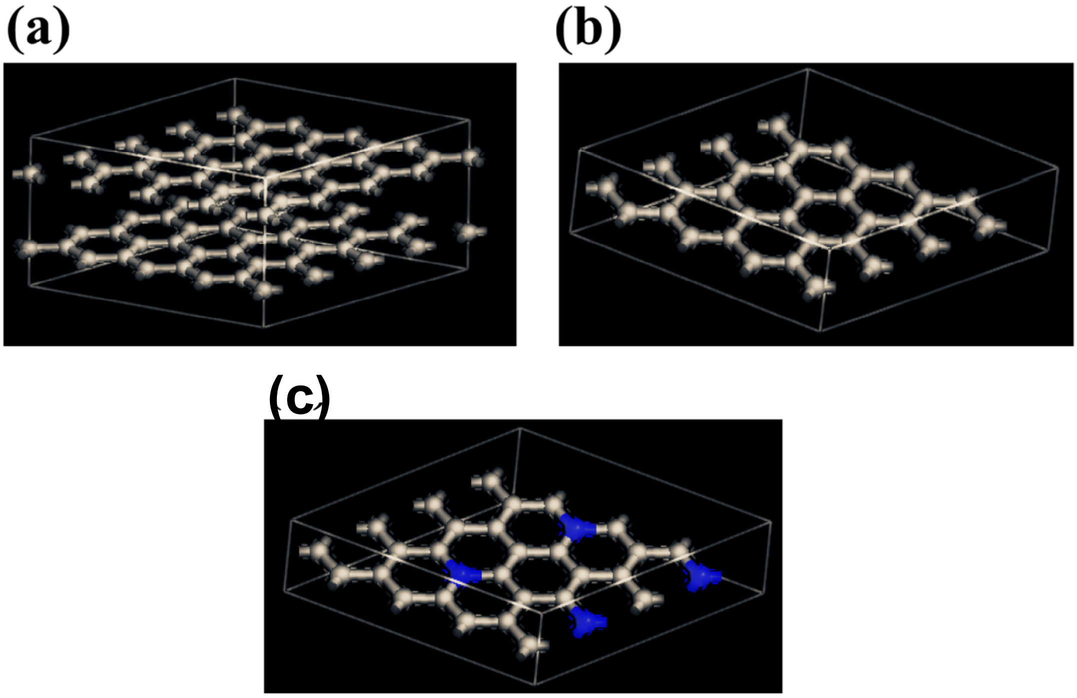

**Fig. S7** The 3D structure of (a) graphite, (b) graphene, and (c) graphitic-N doped graphene. The gray color denotes bond, blue color denotes nitrogen atoms, and metal color denotes atoms.

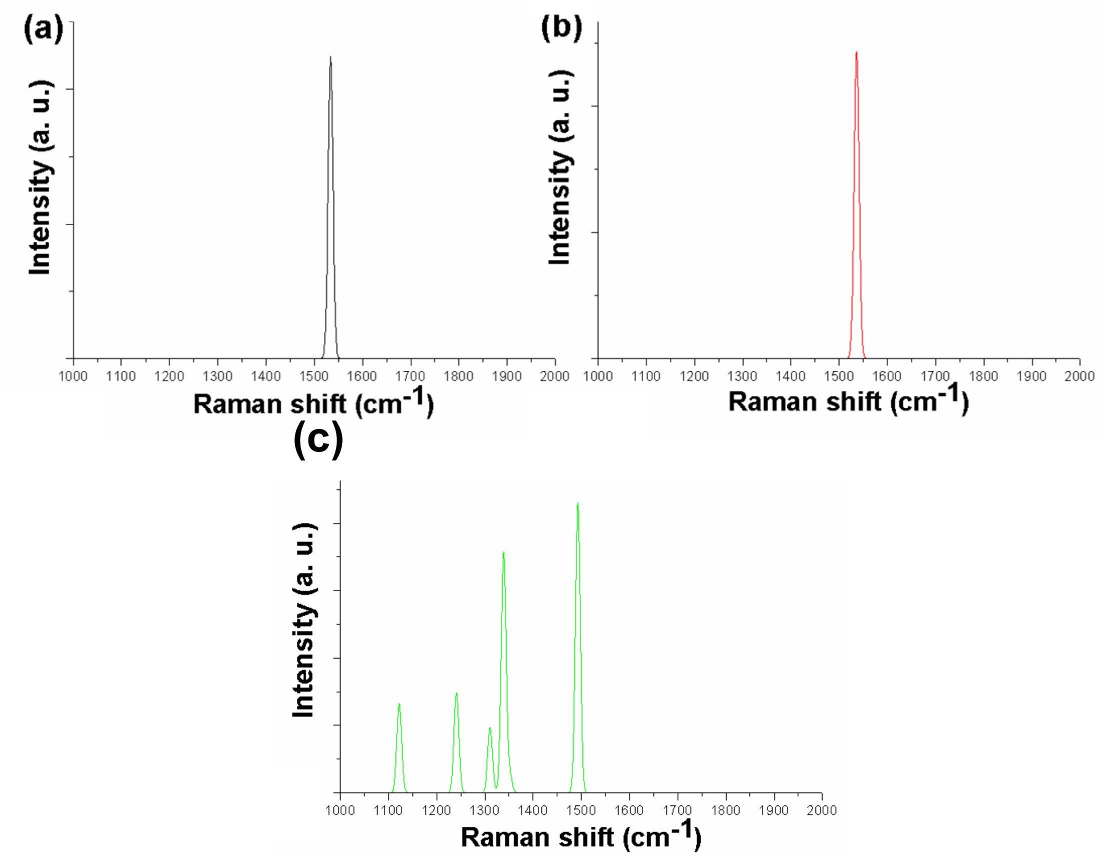

**Fig. S8** Raman shift simulations of (a) graphite, (b) graphene and (c) graphitic N doped graphene based on their 3D structures in Fig. S7.

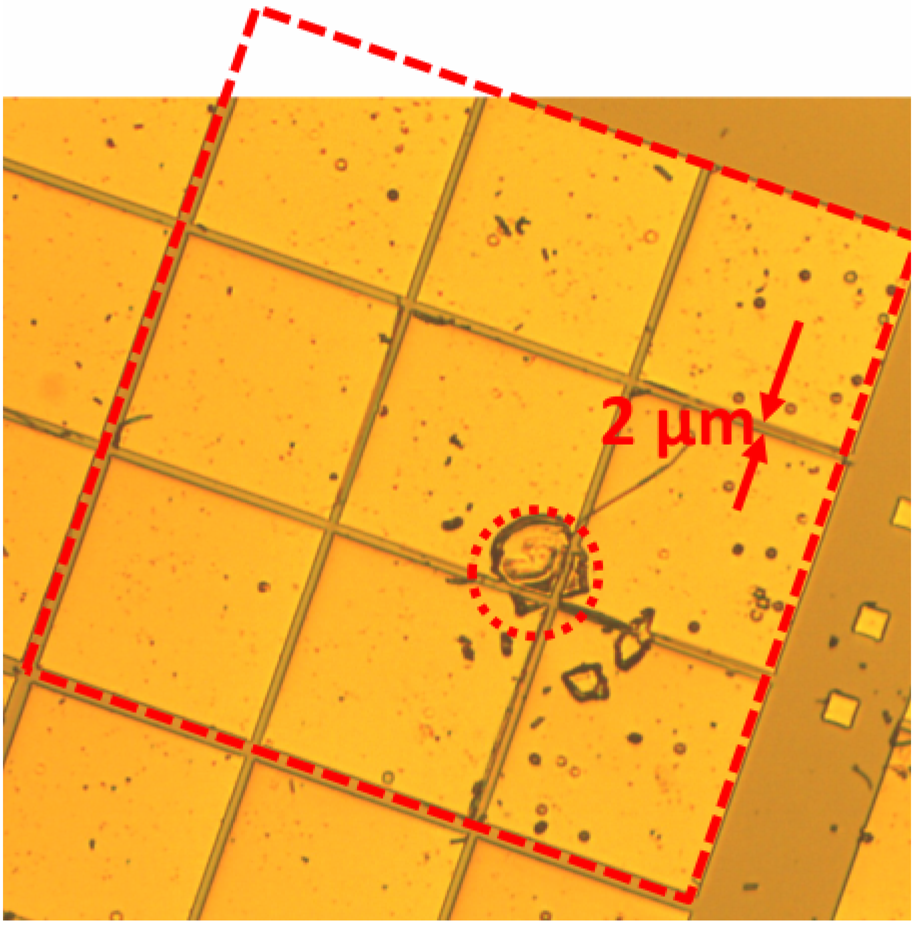

**Fig. S9** (a) AFM image of the NG sheet device used for conductivity measurement.

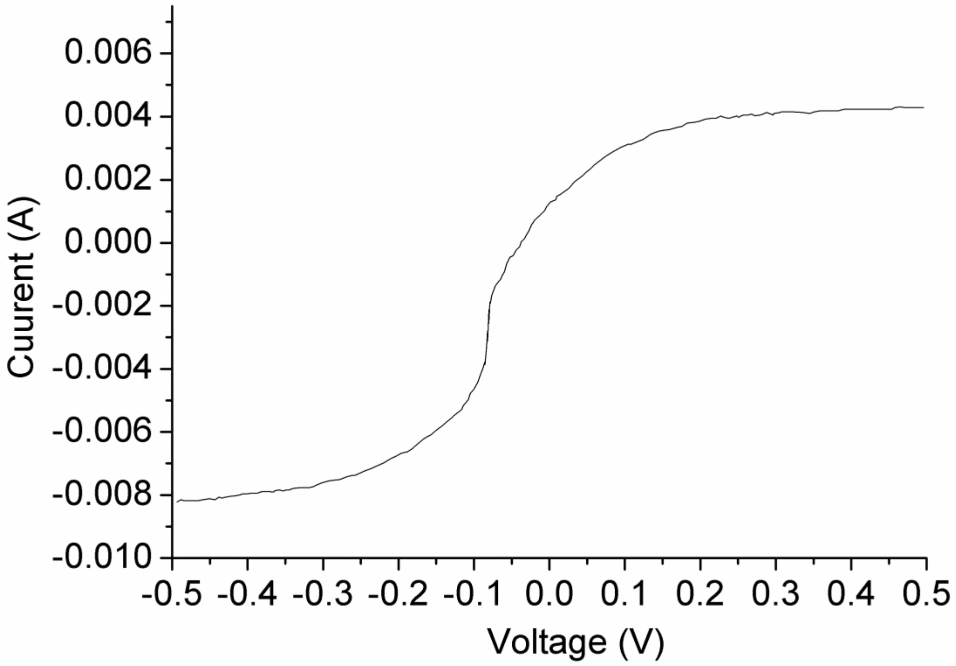

**Fig. S10** The I-V curve of NG synthesized using [Bmim]Br.

According to Ohm's law for circuit theory, the resistance of a material is the applied voltage divided by the current drawn across the material across two electrodes.

$R = V/I$

Where:

R=Resistance (ohms, Ω)

V= Voltage (volts, V)

I = Current (amperes, A)

This electrical resistance is proportional to the sample's length and the resistivity and inversely proportional to the sample's cross sectional area.

$R = \rho \square L/A$

Where:

ρ= Resistivity

A =cross-sectional area (channel length × thickness of graphene sheet)

L = length (graphene sheet width)

$1.167 \times 10^{2} \Omega = \rho \times (30 \mu m)/( 30 \mu m \times 119.9\ nm)$

$\rho = 1.4 \times 10^{-5} \Omega.m$

**Table S2. Conductivity comparison between NG obtained in present work to reported NG and graphene**

| Method | Conductivity (S/m) | Reference |
|---|---|---|
| Thermal treatment | 71500 | Present work |
| Chemical reduction & thermal treatment | 500 | 1 |
| Chemical reduction | 20000 | 2 |
| Flash | 2300 | 3 |
| Chemical reduction | 1000 | 4 |
| Chemical reduction | 0.023 | 5 |
| Thermal treatment | 200 | 6 |
| Chemical reduction | 2300 | 7 |
| Chemical method, Vitamin C | 687 | 8 |
| Chemical method, Vitamin C | 14.1 | 9 |
| Chemical reduction | 800 | 10 |
| Supercritical alcohols | 10638.3 | 11 |
| hybrid Ag–MWNT composite | 57 | 12 |
| Chemical vapour deposition | 500 | 13 |
| CVD | 0.00001 | 14 |
| Liquid Exfoliation | 20000 | 15 |

## References

1 W. Gao, L. B. Alemany, L. J. Ci and P. M. Ajayan, *Nat. Chem.* 2009, **1**, 403-408.

2 Z. J. Fan, W. Kai, J. Yan, T. Wei, L. J. Zhi, J. Feng, Y. M. Ren, L. P. Song and F. Wei, *ACS Nano*, 2010, **5**, 191-198.

3 L. J. Cote, R. Cruz-Silva and J. X. Huang, *J. Am. Chem. Soc.*, 2009, **131**, 11027-11032.

4 Y. Chen, X. Zhang, D. Zhang, P. Yu and Y. Ma, *Carbon*, 2011, **49**, 573-580.

5 S. Stankovich, D. A. Dikin, R. D. Piner, K. A. Kohlhaas, A. Kleinhammes, Y. Jia, Y. Wu, S. T. Nguyen and R. S. Ruoff, *Carbon*, 2007, **45**, 1558-1565.

6 H. C. Schniepp, J. L. Li, M. J. McAllister, H. Sai, M. Herrera-Alonso, D. H. Adamson, R. K. Prud'homme, R. Car, D. A. Saville and I. A. Aksay, *J. Phys. Chem. B*, 2006, **110**, 8535-8539.

7 S. Park, J. An, R. D. Piner, I. Jung, D. Yang, A. Velamakanni, S. T. Nguyen and R. S. Ruoff, *Chem. Mater.*, 2008, **20**, 6592-6594.

8 J. Gao, F. Liu, Y. L. Liu, N. Ma, Z. Q. Wang and X. Zhang, *Chem. Mater.*, 2010, **22**, 2213-2218.

9 J. L. Zhang, H. J. Yang, G. X. Shen, P. Cheng, J. Y. Zhang and S. W. Guo, *Chem. Commun.*, 2010, **46**, 1112-1114.

10 D. R. Dreyer, S. Murali, Y. Zhu, R. S. Ruoff and C. W. Bielawski, *J. Mater. Chem.*, 2011, **21**, 3443–3447.

11 E. B. Nursanto, A. Nugroho, S. A. Hong, S. J. Kim and K. Y. Chung, J. Kim, *Green Chem.*, 2011, **13**, 2714.

12 K. Y. Chun, Y. Oh, J. Rho, J. H. Ahn, Y. J. Kim, H. R. Choi and S. Baik, *Nat. Nanotech.*, 2010, **5**, 853-857.

13 Q. Yu, L. A. Jauregui, W. Wu, R. Colby, J. Tian, Z. Su, H. Cao, Z. Liu, D. Pandey, D. Wei, T. F. Chung, P. Peng, N. P. Guisinger, E. A. Stach, J. Bao, S. S. Pei and Y. P.

Chen, *Nat. Mater.*, 2011, **10**, 443-449.

14 Z. Chen, W. Ren, L. Gao, B. Liu, S. Pei and H. M. Cheng, *Nat. Mater.*, 2011, **10**, 424-428

15 J. N. Coleman, M. Lotya, A. O'Neill, S. D. Bergin, P. J. King, U. Khan, K. Young, A. Gaucher, S. De, R. J. Smith, I. V. Shvets, S. K. Arora, G. Stanton, H. Y. Kim, K. Lee, G. T. Kim, G. S. Duesberg, T. Hallam, J. J. Boland, J. J. Wang, J. F. Donegan, J. C. Grunlan, G. Moriarty, A. Shmeliov, R. J. Nicholls, J. M. Perkins, E. M. Grieveson, K. Theuwissen, D. W. McComb, P. D. Nellist and V. Nicolosi, *Science*, 2011, **331**, 568-571.

16 G. M. Dorris, D. G. Gray, *Cellulose Chem. Technol.*, 1978, **12**, 9-23.